Chemical Hardness as a Possible Diagnostic of the Chaotic Dynamics of Rydberg Atoms in an External Field

P. K. Chattaraj* and S. Sengupta

Department of Chemistry, Indian Institute of Technology, Kharagpur 721 302, India

Received: January 21, 1999; In Final Form: May 12, 1999

The possible signature of chaos in Rydberg atoms has been studied in terms of the dynamic profiles of the chemical hardness (η), polarizability (α), and uncertainty product (V_{ps}). A hydrogen atom in the electronic ground state ($n = 1$) and in an excited electronic state ($n = 15$) behaves differently when placed in both one- and two-color laser pulses. Temporal evolution of η, α, and V_{ps} for these two cases ($n = 1$ and $n = 15$) show marked differences. It appears that a larger V_{ps} and a smaller η value signal a chaotic behavior.

I. Introduction

Chemical hardness[1−3] (η) has turned out to be a cardinal index of molecular structure, reactivity, bonding, and dynamics. Pearson[1] introduced the concept of hardness in the chemistry literature through his famous hard−soft acid−base (HSAB) principle, which can be stated as "hard likes hard and soft likes soft in an acid−base reaction". Density functional theory[3,4] (DFT) has provided the following quantitative definition[5] of hardness for an N-electron system with total energy E and external potential $v(r)$:

$$\eta = \frac{1}{2}\left(\frac{\partial^2 E}{\partial N^2}\right)_{v(r)} \tag{1}$$

Equivalently, it can be expressed as[6]

$$\eta = \int\int \eta(r,r')\, f(r)\, f(r')\, \mathrm{d}r\, \mathrm{d}r' \tag{2a}$$

or as its following approximate version, as suggested by Berkowitz et al.[7]

$$\eta = \frac{1}{N}\int\int \eta(r,r')\, f(r')\, \rho(r)\, \mathrm{d}r\, \mathrm{d}r' \tag{2b}$$

where $f(r)$ is the Fukui function[8,9] and the hardness kernel is defined as[7]

$$\eta(r,r') = \frac{1}{2}\frac{\delta^2 F[\rho]}{\delta\rho(r)\,\delta\rho(r')} \tag{3}$$

where $F[\rho]$ is the Hohenberg−Kohn universal functional[5] of DFT.

Another important electronic structure principle based on the concept of hardness is the maximum hardness principle[1,10] (MHP). The MHP is stated as[10] "there seems to be a rule of nature that molecules arrange themselves so as to be as hard as possible". Formal proofs of both HSAB[6,11] and maximum hardness principles[12] have been furnished using DFT.

The complete characterization of an N-particle system under the influence of the external potential $v(r)$ needs only N and $v(r)$. The response of the system subjected to a change in N at

fixed $v(r)$ can be measured by η. On the other hand, the linear response function[3] takes care of the variation of $v(r)$ at constant N. If the system is acted upon by a weak electric field, polarizability (α) may be used as a measure of the corresponding response. A minimum polarizability principle[13−15] has been proposed, which may be written as "a stable configuration or a favorable process is associated with minimum polarizability".

Dynamics of these reactivity parameters (η and α) have been studied[13,14] in the contexts of various time dependent processes. Whether η and α can provide some insight into the quantum domain behavior of a classically chaotic system is yet to be analyzed. Rydberg atoms and molecules in an oscillating electric field have been considered to be "veritable gold mines for exploring the quantum aspects of chaos".[16] Depending on the frequency and the field intensity, hydrogen[16,17] and helium[18] atoms in the presence of an external field have been shown to exhibit regular/chaotic dynamics. Both quantum fluid dynamics[19,20] (QFD) and quantum theory of motion[21,22] (QTM) have provided quantum signatures of chaos in Rydberg atoms. In QFD[19] the overall motion of the system under consideration is mapped onto that of a "probability fluid" having density $\rho(r,t)$ and current density $j(r,t)$ under the influence of the external classical potential augmented by a quantum potential[19−22] given by

$$v_{qu} = -\left(\frac{\hbar^2}{2m}\right)\frac{\nabla^2 \rho^{1/2}(r,t)}{\rho^{1/2}(r,t)} \tag{4}$$

and $\rho(r,t)$ and $\chi(r,t)$ ($j = \rho\nabla\chi$) are respectively obtained[19−22] from the amplitude and the phase of the wave function. In QTM,[21] a physical system is described in terms of "wave and particle". While the wave motion is governed by the solution to the time dependent Schrödinger equation (TDSE), the particle motion is followed by solving the pertinent Newton equation of motion with forces originating from both classical and quantum potentials. Important insight into the chaotic dynamics has been obtained[20] through ρ versus $-\chi$ plots in QFD, where it has been shown[20] that ρ and $-\chi$ can be considered to be "canonically conjugate". In QTM they are obtained[22] in terms of the distance between two initially close Bohmian trajectories and the associated Kolmogorov−Sinai entropy.

In the present paper we monitor the possible regular/chaotic dynamics through the time evolution of various reactivity indices

---

* Author for correspondence. E-mail address: pkcj@hijli.iitkgp.ernet.in.

Dynamics of Rydberg Atoms in an External Field

J. Phys. Chem. A, Vol. 103, No. 31, 1999 **6123**

of a hydrogen atom in the ground and highly excited electronic states in the presence of one-color and two-color laser pulses. The theoretical background of the present work is provided in section II. Section III presents the numerical details, and the results and discussions are given in section IV. Finally, section V contains some concluding remarks.

II. Theoretical Background

In the present work we study the time evolution of ψ_{1s} and ψ_{15s} wave functions of the hydrogen atom placed in an external oscillating electric field. The pertinent time-dependent Schrödinger equation (in au) in cylindrical polar coordinates $(\tilde{\rho}, z, \phi)$ is

$$\left[-\frac{1}{2} \nabla^2 + v \right] \psi(r,t) = i \frac{\partial \psi(r,t)}{\partial t} \quad (5a)$$

where the potential v is given by

$$v = -\frac{1}{r} + v_{\text{ext}} \quad (5b)$$

In eq 5b the external potential for the monochromatic and bichromatic laser pulses may be written as

$$v_{\text{ext}} = \epsilon \sin(\omega_1 t) z \qquad \text{for monochromatic pulse} \quad (5c)$$

$$= 0.5\epsilon \, [\, \sin(\omega_1 t) + \sin(\omega_2 t)] z$$
$$\text{for bichromatic pulse} \quad (5d)$$

To have a slow oscillation during and after the laser source being switched on, ϵ is written in terms of the maximum amplitude ϵ_0 and the switch-on time t' as

$$\epsilon = \epsilon_0 t/t' \qquad \text{for } 0 \leq t \leq t' \quad (5e)$$

$$= \epsilon_0 \qquad \text{otherwise} \quad (5f)$$

It may be noted that for a many-electron problem one may either solve the associated TDSE or the corresponding generalized nonlinear Schrödinger equation within a quantum fluid density functional framework,[13,14,23] the latter being three-dimensional even in the case of a many-electron system. To construct the hardness kernel (eq 3), we need the Hohenberg−Kohn universal functional $F[\rho]$. For a many-electron system $F[\rho]$ may be taken as[14]

$$F[\rho] = \frac{1}{2} \int \rho(r,t) |\nabla \chi(r,t)|^2 \, dr + T[\rho] +$$
$$\frac{1}{2} \int\int \frac{\rho(r,t)\, \rho(r',t)}{|r - r'|} \, dr \, dr' + E_{\text{xc}}[\rho] \quad (6a)$$

where the first term is the macroscopic kinetic energy, the last term is the exchange-correlation energy, and $T[\rho]$ is the intrinsic kinetic energy given by[14]

$$T[\rho] = T_0[\rho] + T_{\text{w}}[\rho] - a(N)\lambda \int \frac{\rho^{4/3}/r}{1 + \frac{r\rho^{1/3}}{0.043}} \, dr \quad (6b)$$

where $T_0[\rho]$ is the Thomas−Fermi functional,[3] $T_{\text{w}}[\rho]$ is the Weizsäcker functional,[3] λ is a constant,[14] and $a(N)$ is an N-dependent parameter.[14]

For obtaining the global hardness η (eq 2b) we also require the Fukui function $f(r)$. We employ the following local formula for $f(r)$,

$$f(r) = \frac{s(r)}{\int s(r) \, dr} \quad (7a)$$

where the local softness $s(r)$ is given as follows as prescribed by Fuentealba[24]

$$s(r) = \frac{\delta(r - r')}{2\eta(r,r')} \quad (7b)$$

For calculating $\eta(r,r')$ of the above equation the following local form for $F[\rho]$ is used:[14]

$$F^{\text{local}}[\rho] = T^{\text{local}}[\rho] + V_{\text{ee}}^{\text{local}}[\rho] \quad (7c)$$

where the local kinetic energy[25] and the electron−electron repulsion energy[26] may be taken as[14]

$$T^{\text{local}}[\rho] = T_0[\rho] + \frac{3}{4\pi} (3\pi^2)^{1/3} \int \frac{\rho^{4/3}/r}{1 + \frac{r\rho^{1/3}}{0.043}} \, dr \quad (7d)$$

and

$$V_{\text{ee}}^{\text{local}}[\rho] = 0.7937(N - 1)^{2/3} \int \rho^{4/3} \, dr \quad (7e)$$

Note that the above treatment is applicable to many-electron systems and all electron−electron interaction terms would be absent in the case of a hydrogen atom.

To follow the polarizability dynamics the dynamic polarizability is defined as[13,14]

$$\alpha(t) = |D_{\text{ind}}^z(t)|/|\mathcal{F}_z(t)| \quad (8)$$

where $D_{\text{ind}}^z(t)$ is the electronic part of the induced dipole moment and $\mathcal{F}_z(t)$ is the component of the external Coulomb field along the z-axis.

The phase space volume or the uncertainty product, V_{ps}, has been shown[27] to be an important diagnostic of the quantum signature of classical chaos[27] as related to the compactness of the electron cloud.[28] For the present problem it may be defined as

$$V_{\text{ps}} = \{\langle (p_{\tilde{\rho}} - \langle p_{\tilde{\rho}} \rangle)^2 \rangle \langle (p_z - \langle p_z \rangle)^2 \rangle \langle (\tilde{\rho} - \langle \tilde{\rho} \rangle)^2 \rangle \langle (z - \langle z \rangle)^2 \rangle\}^{1/2} \quad (9)$$

A sharp increase in $V_{\text{ps}}(t)$ implies a chaotic motion[27] since it is a measure of the associated quantum fluctuations.[27]

III. Numerical Solution

The TDSE (eq 5) is solved numerically as an initial boundary value problem using an alternating direction implicit method.[29] The solution procedure begins with the ψ_{1s} and ψ_{15s} analytical wave functions of the hydrogen atom. Since the electron density varies rapidly near the nucleus and relatively slowly elsewhere, we transform the variables as follows

$$y = \tilde{\rho}\psi \quad (10a)$$

and

$$\tilde{\rho} = x^2 \quad (10b)$$

6124 *J. Phys. Chem. A, Vol. 103, No. 31, 1999*
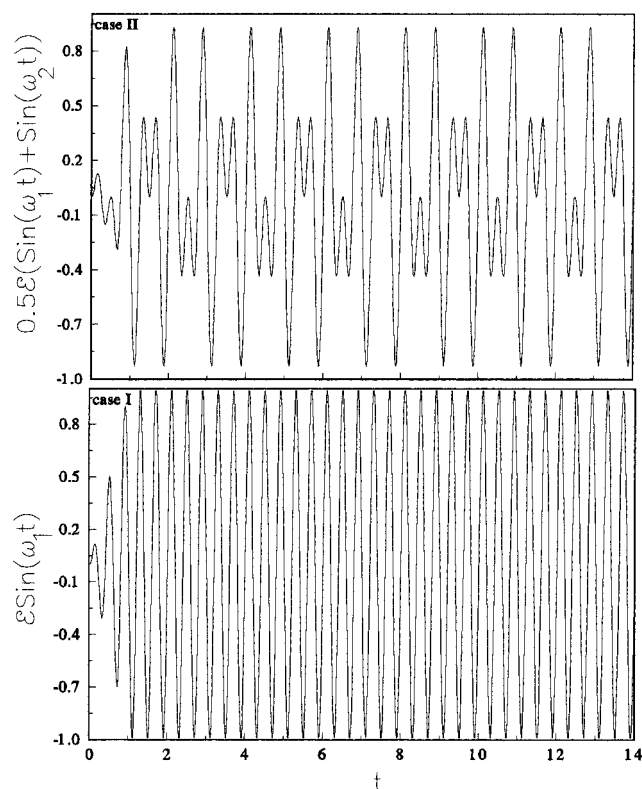
Chattaraj and Sengupta

Figure 1. Time evolution of the external electric field: (I) monochromatic field; (II) bichromatic field.

Eq 5 takes the following form in the transformed variables once an analytical integration is carried out over $0 \leq \phi \leq 2\pi$,

$$\left\{ \left(\frac{3}{4x^3}\right)\frac{\partial y}{\partial x} - \left(\frac{1}{4x^2}\right)\frac{\partial^2 y}{\partial x^2} - \frac{\partial^2 y}{\partial z^2}\right\} - \left(\frac{1}{x^4} - 2v\right)y = 2i\frac{\partial y}{\partial t} \quad (11)$$

The resulting tridiagonal matrix equation is solved using a Thomas algorithm. The mesh sizes adopted here are $\Delta x = \Delta z = 0.4$ au and $\Delta t = 0.01$ au, ensuring the stability of the forward-time-central-space type numerical scheme adopted here.

The initial and boundary conditions associated with this problem are

$$y(x,z) \quad \text{is known for} \quad \forall x,z, \quad \text{at } t = 0 \quad (12a)$$

$$y(0,z) = 0 = y(\infty,z) \quad \forall z,t \quad (12b)$$

$$y(x,\pm\infty) = 0 \quad \forall x,t \quad (12c)$$

The numerical scheme is stable[30] due to the presence of $i = (-1)^{1/2}$. As a further check of the numerical accuracy, we have verified the conservation of the norm and energy (in zero field cases). The wave function is moved forward to the end of the simulation and then taken back to its initial position by reversing the time direction, where the original profile is reproduced well within the tolerance limit of the present calculation. All calculations have been done in double precision. The field parameters are chosen as $\epsilon_0 = 1.0$, $t = 1.0$, $\omega_1 = 5\pi$, and $\omega_2 = 3\pi$. All quantities are in atomic units unless otherwise specified.

IV. Results and Discussion

The time dependence of different quantities are depicted in Figures 1−4. Unless otherwise specified, in all the figures, I and II, respectively, refer to the monochromatic and bichromatic external fields whereas a and b refer to the ψ_{1s} and ψ_{15s} electronic states, respectively, of the hydrogen atom.
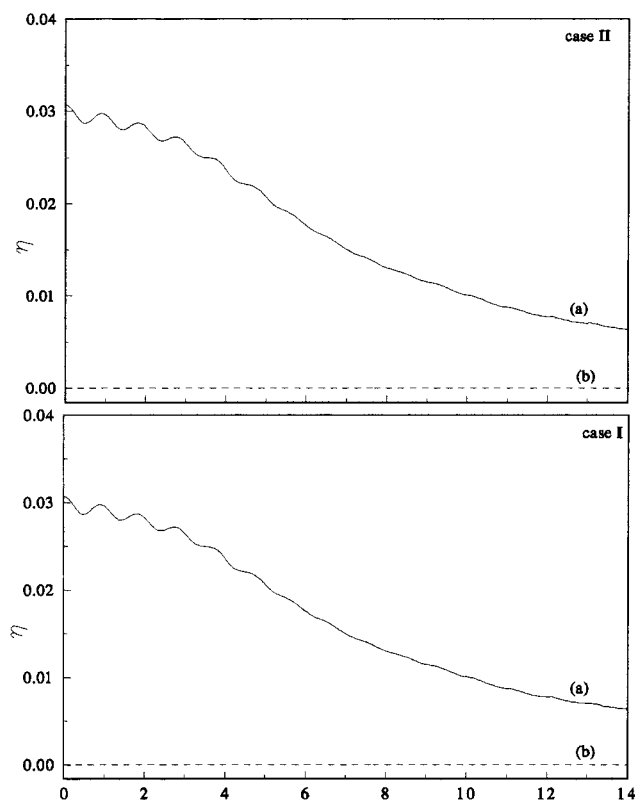

Figure 2. Time evolution of global hardness (η) for a hydrogen atom subjected to (I) a monochromatic electric field (a) with initial state Ψ_{1s} and (b) with initial state Ψ_{15s} or to (II) a bichromatic electric field (a) with initial state Ψ_{1s} and (b) with initial state Ψ_{15s}.

Figure 1 presents the time dependence of the external field, while that of chemical hardness (η) is presented in Figure 2. For both one- and two-color cases η is much larger for the $n = 1$ state than that of the $n = 15$ state for the whole time range. This may be considered to be a dynamical variant of the MHP. Hardness oscillates in time in all the cases. However, the oscillation is neither in phase nor out of phase with respect to the oscillations in the external one- and two-color fields. It is expected because of the fact that as soon as the laser is switched on, there starts a tug-of-war between the atomic nucleus and the external field to govern the electron-density distribution. The nucleus tries to make the density distribution spherically symmetric owing to the central nature of the nuclear Coulomb field while the cylindrical symmetry of the applied electric field tries to create an oscillating dipole that emits radiation including higher harmonics. Overall density oscillation becomes nonlinear due to the interplay of two different types of effects. Both the amplitude and the frequency of oscillation are larger in the two-color situation. Hardness for the $n = 1$ state decreases (for both the cases I and II) and attains a more or less steady value at the end of the simulation, which is still very large in comparison to the corresponding value for the $n = 15$ state. The η values at this point are respectively 0.006 372, 1.91 × 10⁻⁵ and 0.006 368, 1.93 × 10⁻⁵ for the cases Ia,b and IIa,b. For both the cases I and II, η values relative to the corresponding values in absence of the field (not shown) are much larger for the $n = 1$ state. It appears that a relatively smaller η value signals a possible chaotic dynamics.

Polarizability values as they evolve in the course of time are presented in Figure 3. It oscillates with a frequency that is double that of the external field. The extrema in the external field correspond to the minima in α and the latter blows up when
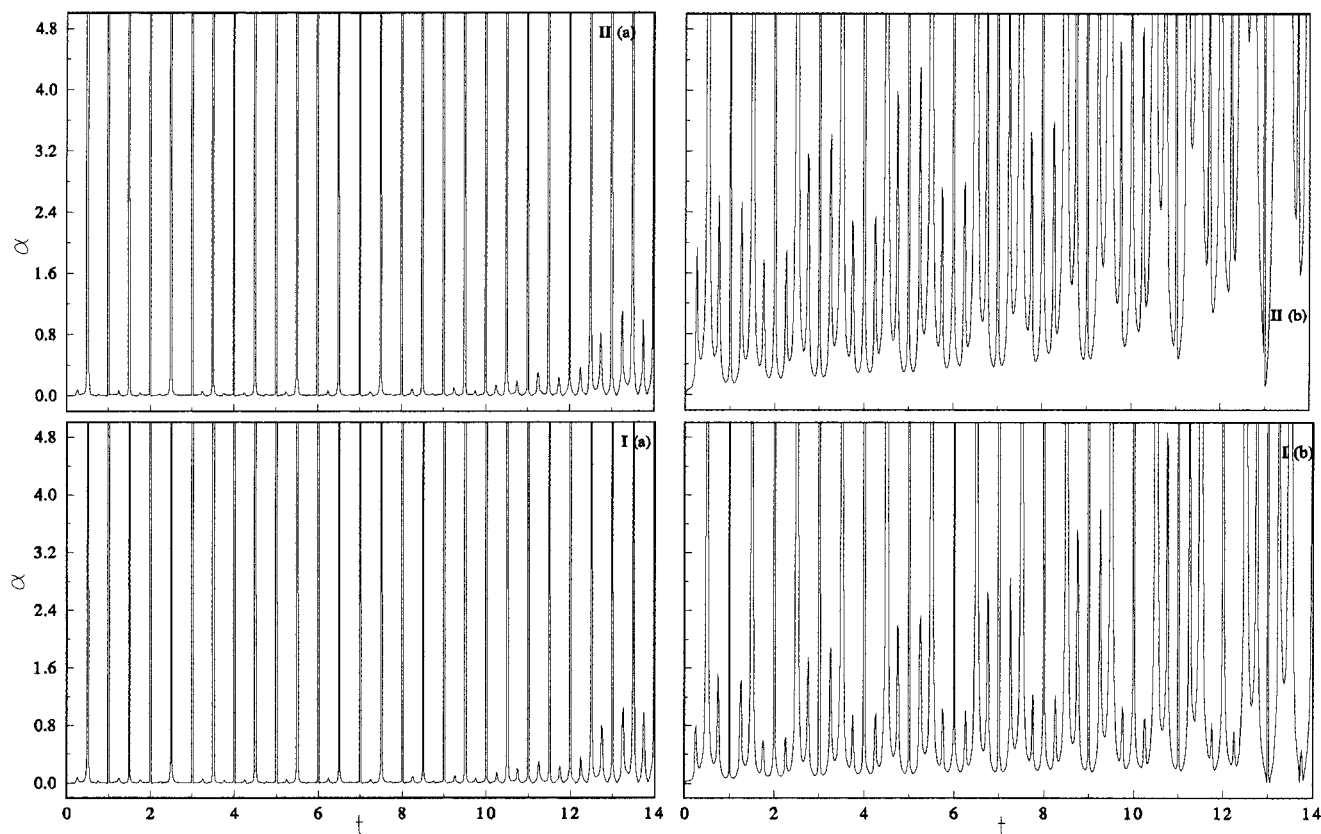
Dynamics of Rydberg Atoms in an External Field

J. Phys. Chem. A, Vol. 103, No. 31, 1999 **6125**

Figure 3. Time evolution of electric polarizability (α) for a hydrogen atom subjected to (I) a monochromatic electric field (a) with initial state Ψ_{1s} and (b) with initial state Ψ_{15s} or to (II) a bichromatic electric field (a) with initial state Ψ_{1s} and (b) with initial state Ψ_{15s}.
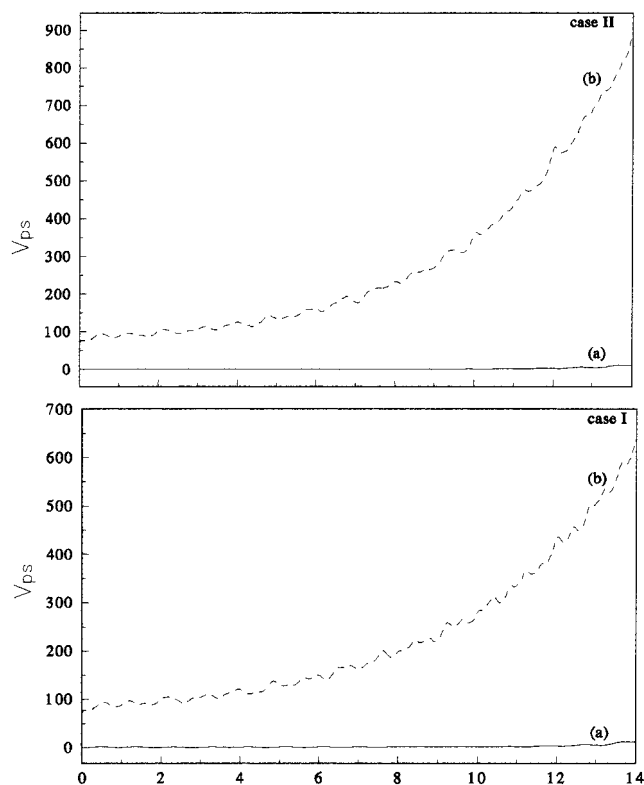

Figure 4. Time evolution of phase volume (V_{ps}) for a hydrogen atom subjected to (I) a monochromatic electric field (a) with initial state Ψ_{1s} and (b) with initial state Ψ_{15s} or to (II) a bichromatic electric field (a) with initial state Ψ_{1s} and (b) with initial state Ψ_{15s}.

the field is zero. The infimum values up to the end of the simulation for the cases Ia,b and IIa,b are respectively 3.91 ×

10^{-5}, 0.01 and 3.99 × 10^{-5}, 0.11. The minimum polarizability principle reveals itself in a time-dependent situation.

Finally, Figure 4 depicts the dynamics of the uncertainty product. As in the case of η, V_{ps} also oscillates neither in phase nor out of phase with the external field. Both the amplitude and the frequency are larger in the two-color case. For the $n = 1$ state V_{ps} retains its initial ($t = 0$) small value whereas for the $n = 15$ state it increases quickly to a very large value. The V_{ps} values for the cases Ia,b and IIa,b at the end of the simulation are 11.54, 638.92 and 11.63, 888.90, respectively. The increase in V_{ps} value is much more in the $n = 15$ state in comparison to that in the $n = 1$ state for both monochromatic and bichromatic cases. Since V_{ps} measures the quantum fluctuations, a chaotic trajectory is generally associated with large V_{ps} values.[27] "...large increases in V_{ps} can be expected to accompany a chaotic trajectory. Conversely, small to moderate increases in V_{ps} can be evidence that given quantum mechanical trajectory should be regarded a nonchaotic".[27a] In general, the electrons are "tightly bound" and hence the distribution is "less diffuse" for the $n = 1$ state and "loosely bound" for the $n = 15$ state and the system is expected to be harder and less polarizable for the ground state.[1–4,15] Again, the electron density being more compact in the ground state, the corresponding uncertainty product is expected[28] to be small. Once the external field is switched on, the ground state density would be distributed over a larger volume and consequently there would be a decrease in η and an increase in α and V_{ps} of the system. Since a smaller η value is accompanied with a larger V_{ps} value and vice versa and V_{ps} is known[27] to bear the signature of the classical chaos in the corresponding quantum domain behavior, hardness can as well be considered to be a diagnostic of the chaotic dynamics in a quantum system. It deserves a thorough study including other quantum chemical problems.

V. Concluding Remarks

Dynamics of a hydrogen atom in its ground state and a highly excited electronic state in the presence of monochromatic and bichromatic laser pulses have been studied in terms of the time evolution of the hardness, polarizability, and uncertainty product. The atom is harder and less polarizable and has a smaller phase volume for the ground state. For both the laser pulses the increase in the uncertainty product for the excited state is very large, which implies a possible chaotic dynamics. A larger hardness value, on the other hand, is expected to characterize a regular behavior.

References and Notes

(1) Pearson, R. G. *Chemical Hardness: Applications from Molecules to Solids*; Wiley-VCH Verlag GMBH: Weinheim, 1997. *Hard and Soft Acids and Bases*; Dowden, Hutchinson and Ross: Stroudsberg, PA, 1973. *Coord. Chem. Rev.* **1990**, *100*, 403.

(2) *Chemical Hardness: Structure and Bonding*; Sen, K. D., Mingos, D. M. P., Eds.; Springer-Verlag: Berlin, 1993; Vol. 80.

(3) Parr, R. G.; Yang, W. *Density Functional Theory of Atoms and Molecules*; Oxford University Press: Oxford, U.K., 1989.

(4) Hohenberg, P.; Kohn, W. *Phys. Rev. B* **1964**, *136*, 864. Kohn, W.; Sham, L. J. *Phys. Rev. A* **1965**, *140*, 1133.

(5) Parr, R. G.; Pearson, R. G. *J. Am. Chem. Soc.* **1983**, *105*, 7512.

(6) Harbola, M. K.; Chattaraj, P. K.; Parr, R. G. *Isr. J. Chem.* **1991**, *31*, 395.

(7) Berkowitz, M.; Ghosh, S. K.; Parr, R. G. *J. Am. Chem. Soc.* **1985**, *107*, 6811. Ghosh, S. K.; Berkowitz, M. *J. Chem. Phys.* **1985**, *83*, 2976.

(8) Fukui, K. *Science* **1982**, *218*, 747.

(9) Parr, R. G.; Yang, W. *J. Am. Chem. Soc.* **1984**, *106*, 4049.

(10) Pearson, R. G. *J. Chem. Educ.* **1987**, *64*, 561; *Acc. Chem. Res.* **1993**, *26*, 250.

(11) Chattaraj, P. K.; Lee, H.; Parr, R. G. *J. Am. Chem. Soc.* **1991**, *113*, 1855.

(12) Parr, R. G.; Chattaraj, P. K. *J. Am. Chem. Soc.* **1991**, *113*, 1854. Chattaraj, P. K.; Liu, G. H.; Parr, R. G. *Chem. Phys. Lett.* **1995**, *237*, 171. For a recent review, see: Chattaraj, P. K. *Proc. Indian Natl. Sci. Acad., Part A* **1996**, *62*, 513.

(13) Chattaraj, P. K.; Sengupta, S. *J. Phys. Chem.* **1996**, *100*, 16126.

(14) Chattaraj, P. K.; Sengupta, S *J. Phys. Chem. A* **1997**, *101*, 7893. Chattaraj, P. K.; Sengupta, S.; Poddar, A. *Int. J. Quantum Chem.* **1998**, *69*, 279. In *Nonlinear Dynamics and Computational Physics*; Sheorey, V. B., Ed.; Narosa: New Delhi, 1999; pp 45−53. In the last two papers $\epsilon \sin(\omega t)$ is plotted against t in Figures 1 and 8, respectively.

(15) Chattaraj, P. K.; Poddar, A. *J. Phys. Chem. A* **1998**, *102*, 9944; *Ibid.* **1999**, *103*, 1274.

(16) Lakshmanan, M.; Ganeshan, K. *Curr. Sci.* **1995**, *68*, 38.

(17) Casati, G.; Chirikov, B. V.; Guarneri, I.; Shepelyansky, D. L. *Phys. Rep.* **1987**, *154*, 77. Hasegawa, H.; Robnik, M.; Wunner, G. *Prog. Theor. Phys. Suppl.* **1989**, *98*, 198. Ganeshan, K.; Lakshmanan, M. *Phys. Rev.* **1990**, *A42*, 3940. Howard, J. E.; Farelly, D. *Phys. Lett.* **1993**, *A178*, 62. Delande, D.; Gay, J.C. *Phys. Rev. Lett.* **1987**, *59*, 1809. Delande, D. *Chaos and Quantum Physics*; Elsevier: Amsterdam, 1991. Friedrich, H.; Wintgen, D. *Phys. Rep.* **1989**, *183*, 37. Holle, A.; Weibusch, G.; Main, J.; Hager, B.; Rottke, H.; Welge, K. H. *Phys. Rev. Lett.* **1986**, *56*, 2594. Holle, A.; Main, J.; Weibusch, G.; Rottke, H.; Welge, K. H. *Phys. Rev. Lett.* **1988**, *61*, 161.

(18) Mariani, D. R.; van de Water, W.; Koch, P. M.; Bergeman, T. *Phys. Rev. Lett.* **1983**, *50*, 1261. van de Water, W.; Yoakum, S.; van Leeuwen, K. A. H.; Sauer, B. E.; Moorman, L.; Galvez, E. J.; Mariani, D. R.; Koch, P. M. *Phys. Rev. A* **1990**,*42*, 573. Sanders, M. M.; Jensen, R. V. *Am. J. Phys.* **1996**, *64*, 1013.

(19) Madelung, E. *Z. Phys.* **1926**, *40*, 322.

(20) Chattaraj, P. K.; Sengupta, S. *Phys. Lett. A* **1993**, *181*, 225; *Ind. J. Pure Appl. Phys.* **1996**, *34*, 518. Chattaraj, P. K. *Ind. J. Pure Appl. Phys.* **1994**, *32*, 101.

(21) Holland, P. R. *The Quantum Theory of Motion*; Cambridge University Press: Cambridge, U.K., 1993.

(22) Sengupta, S.; Chattaraj, P. K. *Phys. Lett. A* **1996**, *215*, 119. Chattaraj, P. K.; Sengupta, S. *Curr. Sci.* **1996**, *71*, 134.

(23) Deb, B. M.; Chattaraj, P. K. *Phys. Rev. A* **1989**, *39*, 1696; *Chem. Phys. Lett.* **1988**, *148*, 550. Deb, B. M.; Chattaraj, P. K.; Mishra, S. *Phys. Rev. A* **1991**, *43*, 1248. Chattaraj, P. K. *Int. J. Quantum Chem.* **1992**, *41*, 845. Chattaraj, P. K. In *Symmetries and Singularity Structures: Intergability and Chaos in Nonlinear Dynamical Systems*; Lakshmanan, M., Daniel, M., Eds.; Springer-Verlag: Berlin, 1990; pp 172−182. Chattaraj, P. K.; Nath, S. *Int. J. Quantum Chem.* **1994**, *49*, 705; *Chem. Phys. lett.* **1994**, *217*, 342.

(24) Fuentealba, P. *J. Chem. Phys.* **1995**, *103*, 6571.

(25) Ghosh, S. K.; Deb, B. M. *J. Phys. B* **1994**, *27*, 381.

(26) Parr, R. G. *J. Phys. Chem.* **1988**, *92*, 3060.

(27) (a) Feit, M. D.; Fleck, J. A., Jr. *J. Chem. Phys.* **1984**, *80*, 2578. (b) Choudhury, S.; Gangopadhayay, G.; Ray, D. S. *Ind. J. Phys.* **1995**, *69B*, 507. (c) Graham, R.; Hohnerbach, M. *Phys. Rev. A* **1991**, *43*, 3966. (d) Idem. *Phys. Rev. Lett.* **1990**, *64*, 637.

(28) Pearson, R. G. *Chemical Hardness: Applications from Molecules to Solids*; Wiley-VCH Verlag GMBH: Weinheim, 1997; pp 116−119.

(29) Ames, W. F. *Numerical Methods for Partial Differential Equations*; Academic: New York, 1977; p 252.

(30) Chattaraj, P. K.; Rao, K. S.; Deb, B. M. *J. Comput. Phys.* **1987**, *72*, 504.